Bulletin of the Seismological Society of America, Vol. 70, No. 1, pp. 283–292, February 1980

TIDAL TILT FROM LOCALIZED OCEAN LOADING IN THE NEW HEBRIDES ARC

BY JEAN-MICHEL MARTHELOT*, ELISABETH COUDERT*, AND BRYAN L. ISACKS

ABSTRACT

Tidal signals recorded by two tiltmeters located near the coast on Vate Island (New Hebrides) are interpreted in terms of the loading effect of the local tide. Homogeneous and stratified elastic models are used in the computation of the theoretical tilts due to the tidal loading. The direction and the magnitude of the tidal tilt recorded at a distance of 120 m from the coast indicate the presence of a surficial layer with a very low value of rigidity overlying materials with much higher rigidity.

INTRODUCTION

During July 1976 Cornell University and the Office de la Recherche Scientifique et Technique Outre-Mer (ORSTOM) established a tiltmeter network on three islands of the New Hebrides island arc (Figure 1; see also Isacks *et al.*, 1978). The network is part of a program to search for aseismic deformations related to the generation of large shallow earthquakes in the New Hebrides zone of lithosphere subduction. The best sites for the tiltmeter stations were found to be near the coast; thus, the stations are located at distances of between 120 m and 2 km from the nearest shorelines. Prominent on some of the records are signals with tidal periodicities. The amplitude of this signal at a station is clearly correlated with the distance between the station and the nearest shoreline. The amplitudes vary from imperceptible to several microradians. The Malapoa station is located closest to the shoreline and records the largest tidal signal. This station also records an oscillatory signal with a period of 25 min produced by a seiche in the embayment of southwest Vate island. These facts indicate that the tidal signals are probably produced by a localized loading of the ocean tides. Takahashi (1929a, b; 1932) and Hagiwara *et al.* (1949, 1951) describe similar effects for tiltmeters located at distances of 22.6 m and 1.2 km from the nearest shoreline. They find that the tidal loading within a radius of 150 m and 50 km, respectively, around the tiltmeter produces the whole tidal signal. They qualitatively interpret the fact that the loading beyond these radii has no effect on the tiltmeters in terms of the effects of crustal stratification.

In this paper the localized loading effect is examined in detail at two stations, Devil's Point and Malapoa, located near the Port Vila tide gauge station (Figure 2). In addition to the classical Boussinesq model of a homogeneous elastic half-space, a model with a layer of low rigidity over a half-space of high rigidity is examined in order to explain the localization of the loading effect. This model is a very simplified version of the multilayered earth model introduced by Farrell (1972) to study regional loading problems in terms of crustal and upper mantle structure.

INSTRUMENTATION AND MEASUREMENTS

Each station consists of a Kinemetrics bubble level tiltmeter coupled to a Rustrack strip chart recorder. Two orthogonal components of the surface tilt are continuously recorded, one parallel to the New Hebrides arc (X), and the other perpendicular to

* Present address: Department of Geological Sciences, Cornell University, Ithaca, New York 14853.

the arc (Y). The X component is oriented along an azimuth of 160° (clockwise from North) and the Y component along 070°. The recording is made at a speed of 0.5 inches/hr and the scale is about 2.2 mm/microradian.

The data of the Port Vila tide gauge have been used to measure the response of the Malapoa and Devil's Point tiltmeters to the tidal fluctuations of water height. There is no phase shift between the tide at Port Vila, the two tilt components at

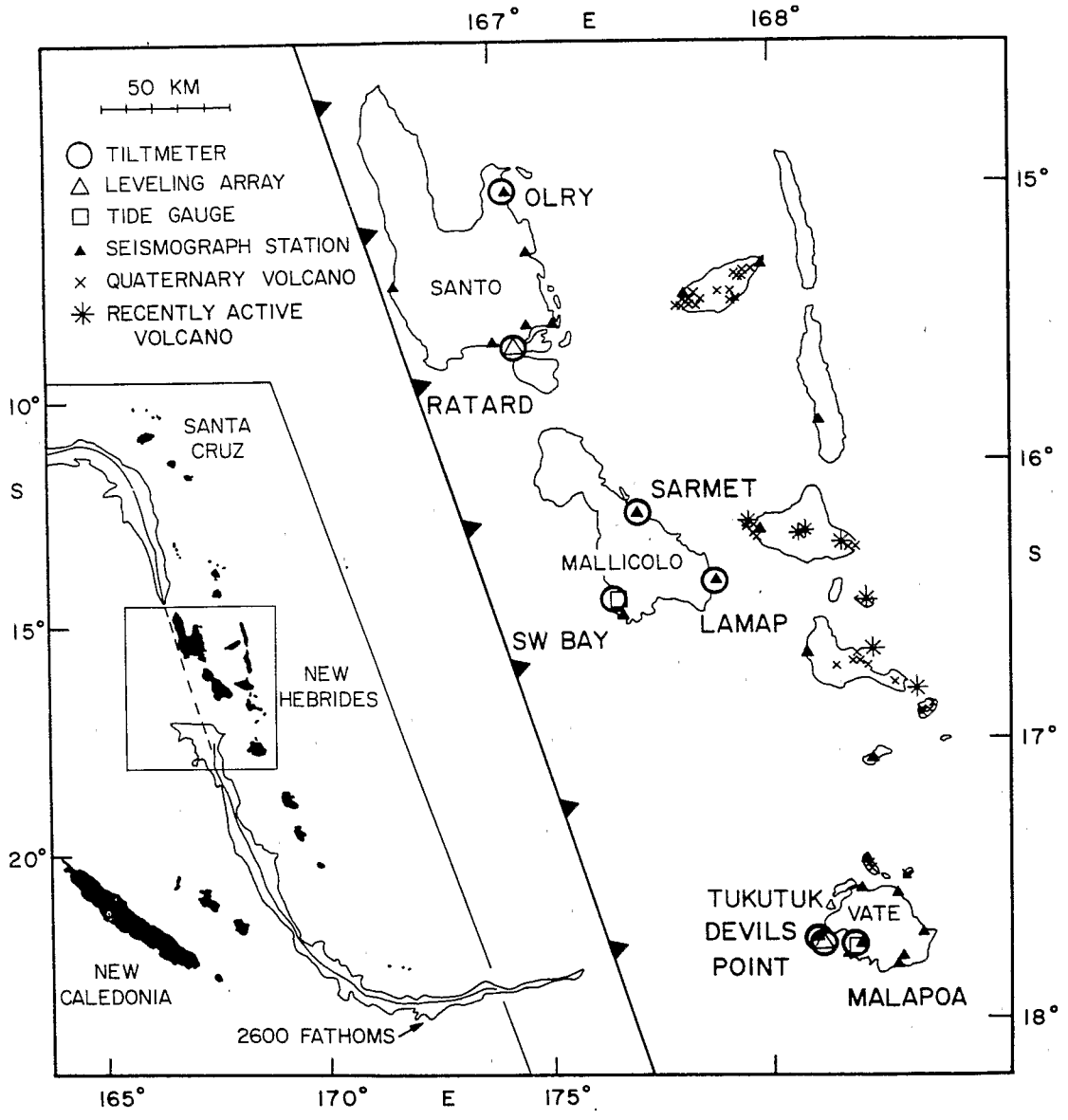

FIG. 1. Map of the central New Hebrides island arc showing the location of tiltmeter stations and instruments used in the joint Cornell-ORSTOM study.

Devil's Point, and the X tilt component at Malapoa. The Y component at Malapoa leads the tide by about 1 hr; as the tidal effect acts mainly on the X component this phase shift is neglected in the following calculation. Table 1 gives the amplitude and direction of the tilt vector at Malapoa and Devil's Point for a water rise of 1 m at Port Vila (see also Figure 3). The uncertainties are due to the approximate calibration of the instruments.

THEORETICAL EFFECT: THE HOMOGENEOUS ELASTIC HALF-SPACE

The solution of the Boussinesq problem in terms of the two orthogonal components, X and Y, of the surface tilt of a homogeneous elastic half-space with vertical loading forces confined to an annulus sector is classical (see, for instance, Zschau,

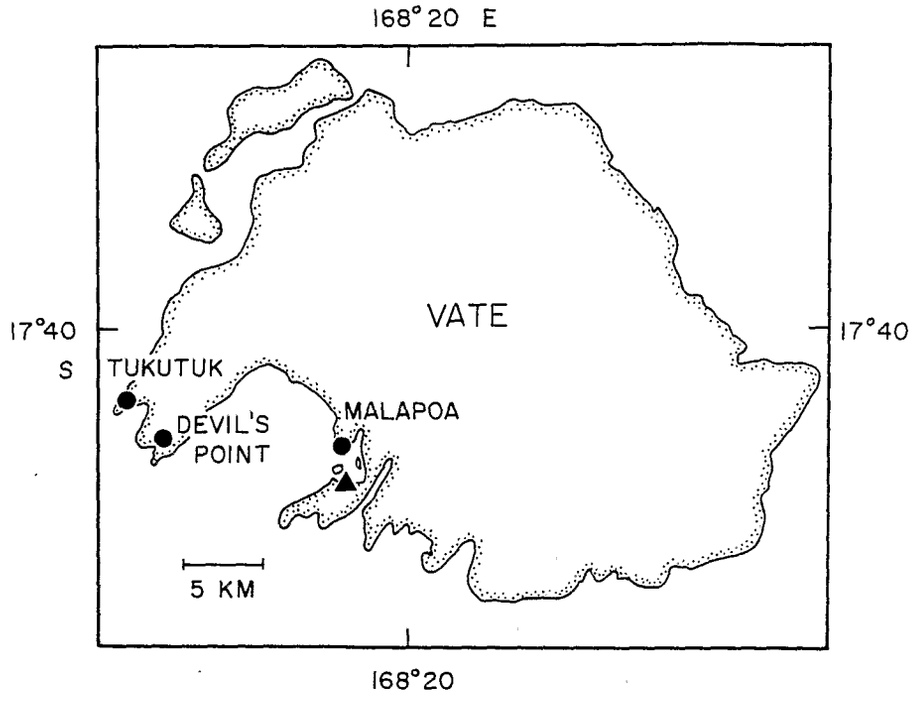

FIG. 2. Map of Vate Island showing the location of the tide gauge in the Port Vila Bay (shown by a triangle) and the tiltmeters at Malapoa, Devil's Point, and Tukutuk.

TABLE 1

AMPLITUDE AND DIRECTION OF THE SURFACE TILT MEASURED FOR A WATER RISE OF 1 m IN PORT VILA.*

Station	Distance to Ocean (m)	Amplitude (μrad)	Azimuth (deg)
Malapoa	120	3.5 ± 0.3	174 ± 4
Devil's Point	700	0.5 ± 0.1	232 ± 8

* Tilt downward in the direction of the specified azimuth is positive. Azimuth is measured in degrees clockwise from North.

1976). The data from Service Hydrographique de la Marine (Noumea, New Caledonia) reveal that the tide has nearly the same phase and magnitude around Vate. Thus, calculation of the local tidal loading tilt is performed by adding in radial increments around the station the effects of successive annulus sectors, distributed according to the shape of the shoreline. Figures 4 and 5 show the result of this calculation at Malapoa and Devil's Point; the azimuths of the observed tilts are also indicated. The ratio of the calculated magnitude of tilt for a given radius of load to the observed magnitude of tilt yields an apparent rigidity coefficient as a function of that radius if it is assumed that the effect of the water mass beyond that radius is negligible (Figure 6).

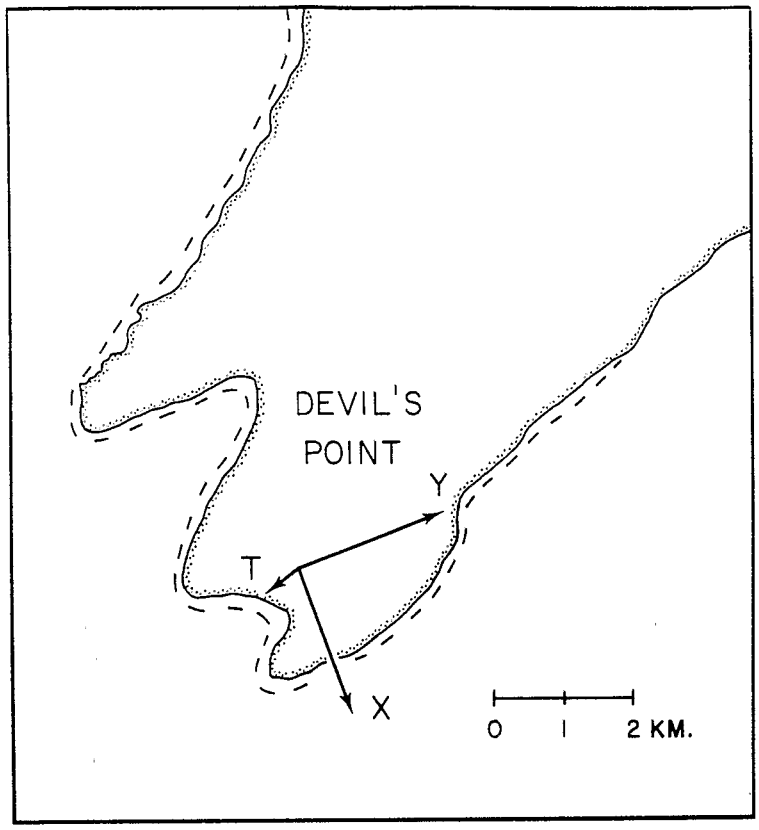

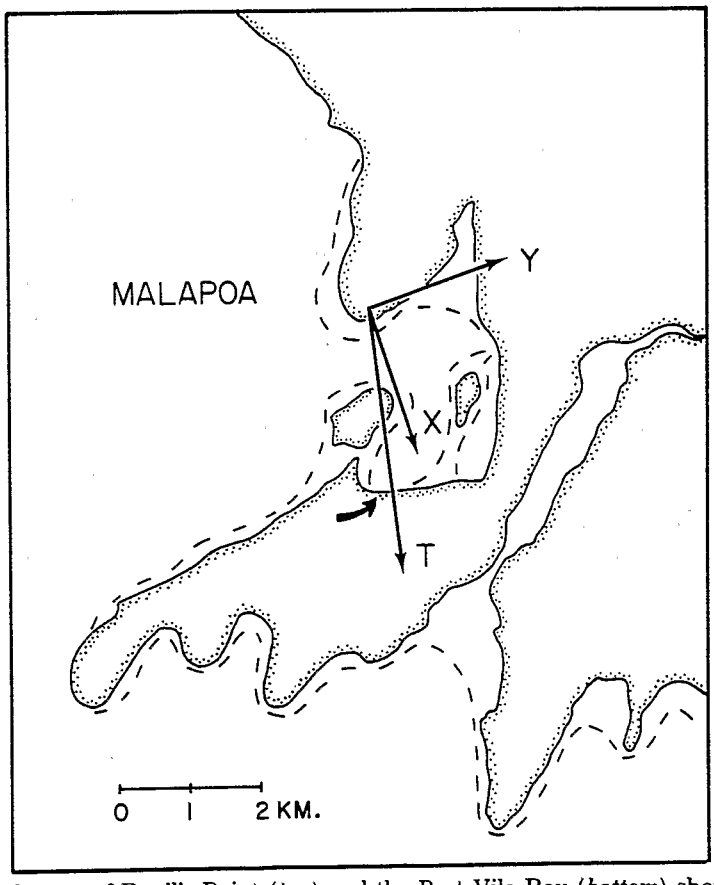

FIG. 3. Detailed maps of Devil's Point (*top*) and the Port Vila Bay (*bottom*) show the directions of the two components X and Y of the tiltmeters; the tilt T resulting from a tidal water rise of 1 m (tilt is downward toward the arrow and the tilt magnitude scale is the same for both cases); the location of the

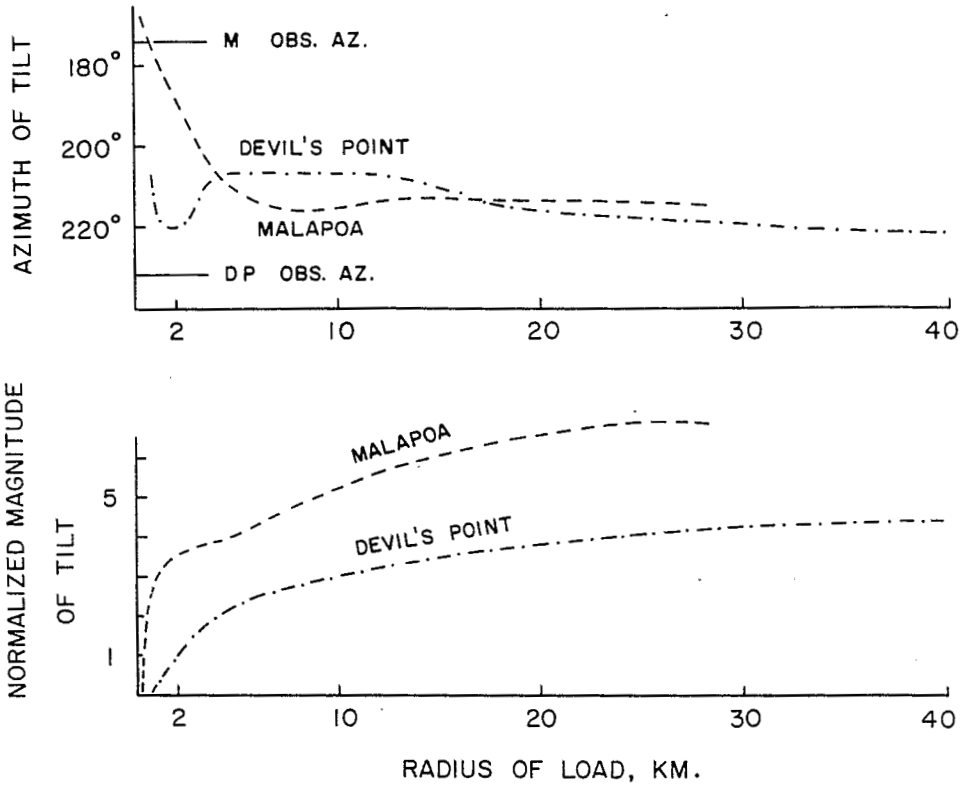

FIG. 4. *Top*: Azimuth (measured clockwise from North) of the calculated tilt versus the radius of the loaded sector. Also shown are the azimuth of the observed tidal tilt at Malapoa and Devil's Point. *Bottom*: $(8\pi\mu/3\rho g h) \times$ magnitude of the calculated tilt versus the radius of the loaded sector; μ is the half-space rigidity, ρ the water density, g the acceleration of gravity, and h the tidal height.

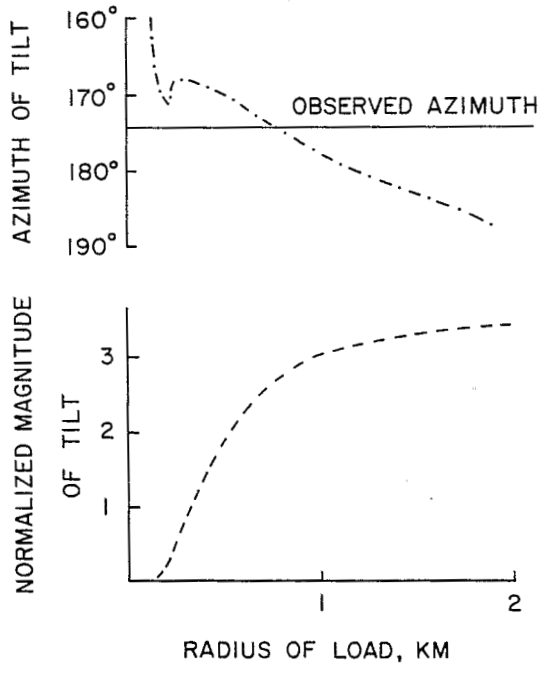

FIG. 5. Detail of Figure 4 for the two first kilometers of the radius of load at Malapoa.

The misfit between the calculated and the observed direction of tilt at Devil's Point is not significant compared to the accuracy of measurement. Thus the homogeneous model can explain the tidal signal at Devil's Point with a rigidity of 10^{10} N/m^2. However, it is not possible to determine the maximum radius within which the loading effect actually acts around the tiltmeter since the misfit between the calculated and the observed direction does not increase with this radius. On the contrary, the observed tilt direction at Malapoa indicates that the loading effect acts only within a maximum radius of about 1 km around that tiltmeter. This fact is inconsistent with the homogeneous model; it indicates that the effective rigidity must increase for the more distant loading. Thus it is reasonable to consider a stratified half-space model in which rigidity increases with depth.

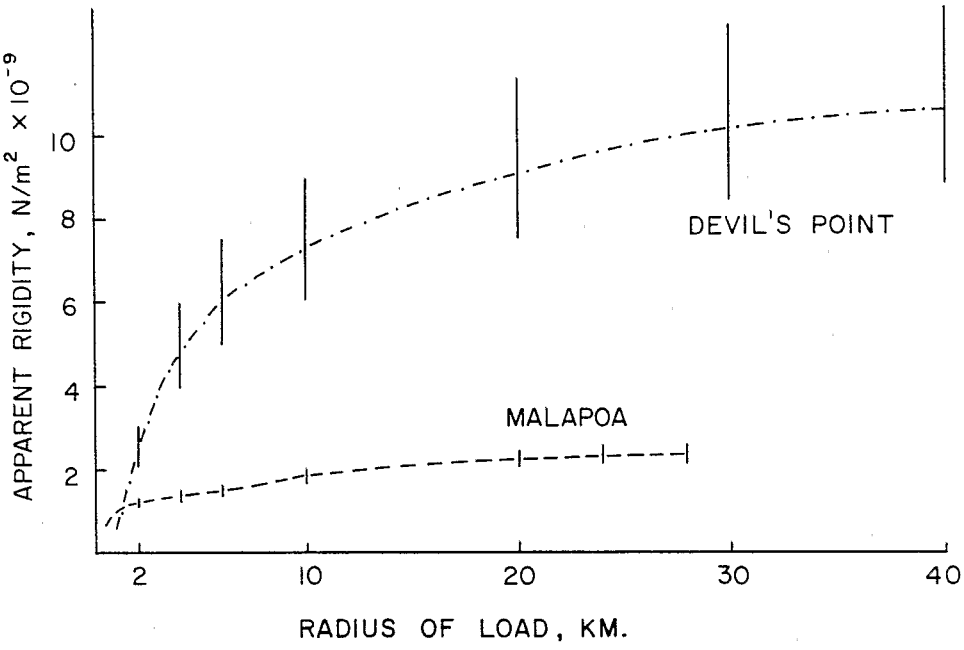

FIG. 6. Apparent rigidity versus the maximum radius within which the tidal loading acts. Error bars are estimates of errors of the measurements.

THE STRATIFIED ELASTIC HALF-SPACE

The solution to the problem of loading of an elastic stratified half-space is obtained by numerical integration (see Appendix). We have performed the calculation for a model with a low-rigidity layer with thickness H overlying a homogeneous half-space with a rigidity coefficient 4.5 times as large as that of the layer. Figure 7 compares the tilt magnitude due to a uniform pressure acting on a quadrant sector from a distance of 120 m from the tiltmeter to a variable distance plotted along the x axis. Two cases are considered for the stratified model, one with $H = 0.5$ km, and the other with $H = 1$ km. Two homogeneous models are also considered, one with rigidity of unity and the other with a rigidity of 4.5. This figure shows that the stratified model responds like the homogeneous model with low rigidity if the load is applied at a distance less than H and like the homogeneous model with high rigidity if the load is applied at a distance larger than H. This is a very good approximation except near H. Adopting this approximate method to perform the calculation leads to a maximum error of only 5 per cent.

Applying the stratified model to the Malapoa results we find that for a thickness H between 0.5 and 1 km a ratio of rigidity equal to 5 reduces the misfit between the calculated and observed direction to 15° while a ratio equal to 10 reduces it to 8°. In this last model, the magnitude of the tilt is accounted for by a rigidity of the surficial layer of about 10^9 N/m^2. Kulhawy (1975) reviews the available data on the Young's modulus and the Poisson's ratio of near-surface materials tested under uniaxial conditions. His results imply a range of the rigidity coefficient of from 4×10^8 N/m^2 to 4×10^{10} N/m^2. Malapoa is located on uplifted coral reef material of unknown thickness. The coral rock consists of reef material, reef talus and lagoonal facies in various degrees of both lithification and solution. It is likely to be quite porous and

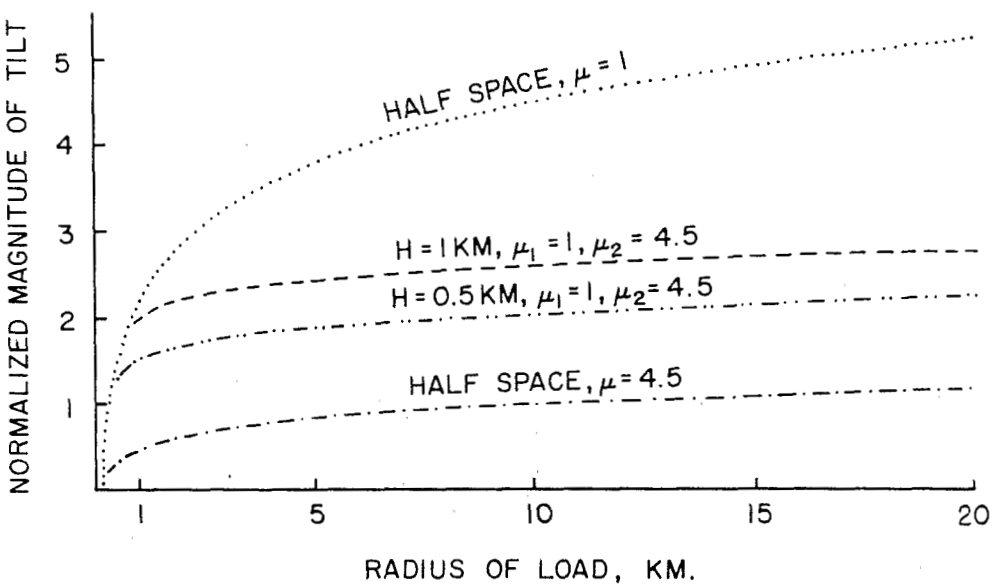

FIG. 7. $(8\pi/3\rho gh) \times$ magnitude of the tilt versus the radius of the loaded quadrant sector for a stratified elastic model (with a layer of rigidity μ_1 and thickness H over a half-space of rigidity μ_2) and for an elastic half-space with rigidity μ.

heterogeneous in structure; it could conceivably have a very low bulk rigidity. Takahashi (1929a) found a similarly low surficial apparent rigidity (1.4×10^9 N/m^2) for a near-shore tiltmeter located on tuff.

The fact that a homogeneous model accounts for the tidal signal recorded at Devil's Point is not inconsistent with the presence of a low rigidity layer with a thickness between 0.5 and 1 km. Devil's Point is at a distance from the shore about equal to the presumed thickness of this layer. Thus the loading effect is mainly due to the lower half-space. Moreover, the rigidity of the homogeneous model which fits the Devil's Point results is equal to the rigidity of the lower half-space at Malapoa if the rigidity ratio for the stratified model is 10.

CONCLUSIONS

Comparison of the tidal tilt signals recorded at two stations on Vate Island with calculations of the tilt produced by ocean loading on a homogeneous or on a stratified elastic half-space leads to the following conclusions.

First, the signal with tidal periodicities recorded at Devil's Point, at a distance of 700 m from the shore, has a direction and a magnitude which agree with the

calculated ones for both the homogeneous and the stratified models. Second, the tidal signal recorded at Malapoa at 120 m from the shore, has a magnitude seven times as large as that at Devil's Point. Its direction implies a very strong increase in rigidity at a depth between 0.5 and 1.0 km. A near-surface layer with the low value of rigidity of 10^9 N/m^2 can account for the observed magnitude.

The porosity of the coral material may also allow the load to percolate closer to the tiltmeter than the shoreline (Frohlich *et al.*, 1975). Evidence for possible complexities of this sort includes the phase shift of about 1 hr between the Y (ENE) component of the Malapoa tiltmeter and the Port Vila tide gauge and the suggestion of a non-sinusoidal waveform of the phase-shifted component. However, the major part of the signal is contributed by the other tiltmeter component X (SSE) which produces a clean sinusoidal signal closely in phase with the local water tides.

Acknowledgments

We wish to thank G. Hade, R. Campillo, J-L. Saos, and J. Laurent for their essential contributions to the installation and maintenance of the tiltmeter network in the New Hebrides; B. Pontoise, M. Larue, J. Recy, and J. Dubois for helpful discussions and criticisms; and D. Citron for drafting the figures. E. Coudert would like to thank ORSTOM for its hospitality during her stay in Noumea.

Appendix

We adopt the method suggested by Farrell (1972). Suppose an elastic half-space including a layer with thickness H and Lame parameters λ and μ, overlying the volume $z \leqq 0$ with Lame parameters λ' and μ'. Call $\sigma = \lambda + 2\mu$, $\eta = \lambda + \mu$, $\kappa = \lambda + 3\mu$. Let us suppose, in cylindrical coordinates, $u(z, r)$ the z-component of the displacement, $v(z, r)$ the radial component, and their Hankel transform $U(z, \xi)$ and $V(z, \xi)$

$$u(z, r) = \int_0^\infty U(z, \xi) J_0(\xi r) \xi \, d\xi$$

$$v(z, r) = \int_0^\infty V(z, \xi) J_1(\xi r) \xi \, d\xi$$

and likewise $T_{zz}(z, \xi)$ and $T_{rz}(z, \xi)$ the transform of order 0 and 1 of the τ_{zz} and τ_{rz} stresses. The elastic equilibrium equation and the stress-strain relationships, when transformed, lead to a first-order system of which the general solutions are in matrix form

$$\begin{bmatrix} U \\ V \\ T_{zz} \\ T_{rz} \end{bmatrix} = \begin{bmatrix} 1 & -\xi z + \kappa/\eta & 1 & \xi z + \kappa/\eta \\ -1 & \xi z & 1 & \xi z \\ 2\mu\xi & -2\mu\xi(\xi z - \sigma/\eta) & -2\mu\xi & -2\mu\xi(\xi z + \sigma/\eta) \\ -2\mu\xi & 2\mu\xi(\xi z - \mu/\eta) & -2\mu\xi & -2\mu\xi(\xi z + \mu/\eta) \end{bmatrix} \begin{bmatrix} Ae^{\xi z} \\ Be^{\xi z} \\ Ce^{-\xi z} \\ De^{-\xi z} \end{bmatrix} . \quad (1)$$

In each layer, the coefficients A, B, C, D are determined by the boundary conditions: displacements and stresses vanishing as $z - > -\infty$; continuity of U, V, T_{zz}, T_{rz} at $z = 0$; at the free surface $z = H$, $\tau_{rz} = 0$ and $\tau_{zz} = \delta(0)$. These conditions

lead to the system

$$\begin{bmatrix} 1 & \kappa/\eta & 1 & \kappa/\eta & -1 & -\kappa'/\eta' \\ -1 & 0 & 1 & 0 & 1 & 0 \\ \mu & \mu\sigma/\eta & -\mu & -\mu\sigma/\eta & -\mu' & -\mu'\sigma'/\eta' \\ -\mu & -\mu^2/\eta & -\mu & -\mu^2/\eta & \mu' & \mu'^2/\eta' \\ e^{\xi H} & -(\xi H - \sigma/\eta)e^{\xi H} & -e^{-\xi H} & -(\xi H + \sigma/\eta)e^{-\xi H} & 0 & 0 \\ -e^{\xi H} & (\xi H - \mu/\eta)e^{\xi H} & -e^{-\xi H} & -(\xi H + \mu/\eta)e^{-\xi H} & 0 & 0 \end{bmatrix} \begin{bmatrix} A \\ B \\ C \\ D \\ E \\ F \end{bmatrix} = \begin{bmatrix} 0 \\ 0 \\ 0 \\ 0 \\ -1/4\pi\mu\xi \\ 0 \end{bmatrix}.$$

Resolving this system, A, B, C, D in the upper layer is obtained; equation (1) leads then to the vertical surface displacement transform

$$\begin{aligned} U(H, \xi) = \{-\sigma/4\pi\mu\eta\xi\}\{[(\mu + \mu'\kappa/\eta)(\mu + \mu'\eta'/\kappa')e^{2\xi H} \\ + (\mu + \mu'\eta'/\kappa')(\mu - \mu')4\xi H \\ - (\mu - \mu'\kappa\eta'/\eta\kappa')(\mu - \mu')e^{-2\xi H}]/[(\mu + \mu'\kappa/\eta)(\mu + \mu'\eta'/\kappa')e^{2\xi H} \\ - (\mu + \mu'\eta'/\kappa')(\mu - \mu')4\xi^2 H^2 - (\mu - \mu')(\mu + \mu'\eta'/\kappa') \\ - (\mu + \mu'\kappa/\eta)(\mu - \mu'\kappa\eta'/\eta\kappa') \\ + (\mu - \mu')(\mu - \mu'\kappa\eta'/\eta\kappa')e^{-2\xi H}]\}. \end{aligned}$$

The asymptotic form of $U(H, \xi)$ is $U^*(H, \xi) = -\sigma/4\pi\mu\eta\xi$, the homogeneous half-space vertical displacement transform. Thus

$$u(H, r) = u^*(H, r) + \int_0^M (U - U^*)(H, \xi) J_0(\xi r)\xi \, d\xi$$

where $(U - U^*)(H, \xi)$ is equivalent to $\exp(-2\xi H)$. The tilt Green function is calculated in the following form

$$\frac{du}{dr}(H, r) = 3/8\pi\mu r^2 + \int_0^M (U - U^*)(H, \xi) J_1(\xi r)\xi^2 \, d\xi$$

References

Farrell, W. E. (1972). Deformation of the earth by surface loads, *Rev. Geophys. Space Phys.* **10,** 761–797.

Frohlich, C., M. W. Major, and B. L. Isacks (1975). Strainmeter and tiltmeter measurements from the Tonga island arc, *Bull. Seism. Soc. Am.* **65,** 563–579.

Hagiwara, T., T. Rikitake, K. Kasahara, and J. Yamada (1949). Observations of the deformation of the Earth's surface at Aburatsubo, Miura Peninsula, Part II and III, *Bull. Earthquake Res. Inst., Tokyo Univ.* **27,** 35–44.

Hagiwara, T., K. Kasahara, J. Yamada, and S. Saito, (1951). Observations of the deformation of the Earth's Surface at Aburatsubo, Miura Peninsula, Part IV, *Bull. Earthquake Res. Inst., Tokyo Univ.* **29,** 455–468.

Isacks, B. L., G. Hade, R. Campillo, M. Bevis, D. Chinn, J. Dubois, J. Recy, and J. L. Saos (1978). Measurements of tilt in the New Hebrides Island Arc, in Proceedings of Conference VII, Stress and Strain Measurements Related to Earthquake Prediction, *U.S. Geol. Surv., Open File Rept.* 79370 176–221.

Kulhawy, F. H. (1975). Stress deformation properties of rock and rock discontinuities, *Eng. Geol.* **9,** 327–350.

Takahashi, R. (1929a). Tilting motion of the earth crust caused by tidal loading, *Bull. Earthquake Res. Inst., Tokyo Univ.* **6,** 85–108.

Takahashi, R. (1929b). Tilting motion of the earth crust caused by secondary undulations of tides in a bay, *Bull. Earthquake Res. Inst., Tokyo Univ.* **7,** 95–102.

Takahashi, R. (1932). Tilting motion of the earth crust observed at Ryozyun (Port Arthur), *Bull. Earthquake Res. Inst., Tokyo Univ.* **10,** 531–559.

Zschau, J. (1976). Tidal sea load tilt of the crust and its application to the study of crustal and upper mantle structure, *Geophys. J.* **44,** 577–593.

OFFICE DE LA RECHERCHE SCIENTIFIQUE ET
TECHNIQUE OUTRE-MER
BPA5
NOUMEA, NEW CALEDONIA (J.M.M.)

DEPARTMENT OF GEOLOGICAL SCIENCES
CORNELL UNIVERSITY
ITHACA, NEW YORK 14853 (B.L.I.)

LABORATOIRE DE GEOPHYSIQUE
UNIVERSITE DE PARIS—SUD
91405 ORSAY, FRANCE (E.C.)

Manuscript received June 25, 1979